Inorganic Chemistry

Article

pubs.acs.org/IC

THF Exchange and Molecular Dynamics in the Series (BDI)MgX(THF), Where X = Bu^n, NEt_2, and OBu^t and BDI = 2-[(2,6-Diisopropylphenyl)amino]-4-[(2,6-diisopropylphenyl)imino]pent-2-ene

Malcolm H. Chisholm,* Kittisak Choojun, Albert S. Chow, Gideon Fraenkel,* and Judith C. Gallucci

Department of Chemistry and Biochemistry, The Ohio State University, 100 West 18th Avenue, Columbus, Ohio 43210, United States

Supporting Information

ABSTRACT: The complexes (BDI)MgX(THF), where X = Bu^n, NEt_2, and OBu^t, are shown to undergo THF exchange at low added concentrations of THF by a dissociative mechanism: X = Bu^n, $\Delta H^{\#}$ (kcal mol^{-1}) = 13.4 ± 0.4 and $\Delta S^{\#}$ (cal mol^{-1} K^{-1}) = 6.3 ± 1.6; X = NEt_2, $\Delta H^{\#}$ (kcal mol^{-1}) = 15.2 ± 0.5 and $\Delta S^{\#}$ (cal mol^{-1} K^{-1}) = 11.4 ± 2.3; X = OBu^t, $\Delta H^{\#}$ (kcal mol^{-1}) = 16.4 ± 0.3 and $\Delta S^{\#}$ (cal mol^{-1} K^{-1}) = 9.5 ± 1.3. The apparent aryl group rotations involving the BDI ligands have, within experimental error, the same activation parameters as the THF dissociation, which suggests that the two are correlated involving a three coordinate reactive intermediate akin to what is well-known for related (BDI)ZnR compounds involving three-coordinate trigonal planar Zn^{2+}. At higher concentrations of THF for X = Bu^n and OBu^t, but not for X = NEt_2, the coalescence temperatures for apparent aryl group rotation are depressed from those of the pure compounds in toluene-d_8, and evidence is presented that this correlates with an associative interchange process which becomes dominant in neat THF. We estimate the I_a mechanism to have activation parameters: $\Delta H^{\#}$ (kcal mol^{-1}) = 5.4 ± 0.1 and $\Delta S^{\#}$ (cal mol^{-1} K^{-1}) = −20.9 ± 0.3 for X = Bu^n and $\Delta H^{\#}$ (kcal mol^{-1}) = 8.3 ± 0.8 and $\Delta S^{\#}$ (cal mol^{-1} K^{-1}) = −19.8 ± 3.0 for X = OBu^t. For the complex (BDI)MgBu^n(2-MeTHF), the dissociative exchange with added 2-MeTHF occurs more readily than for its THF analogue, as expected for the more sterically demanding Lewis base O-donor: $\Delta H^{\#}$ (kcal mol^{-1}) = 12.8 ± 0.5 and $\Delta S^{\#}$ (cal mol^{-1} K^{-1}) = 8.6 ± 1.8. At very low temperatures in toluene-d_8, restricted rotation about the Mg−O(THF) bond is observed for the complexes where X = NEt_2 and OBu^t but not for the complex where X = Bu^n. These observations, which have been determined from dynamic NMR studies, are correlated with the reactivities of these complexes in solution.

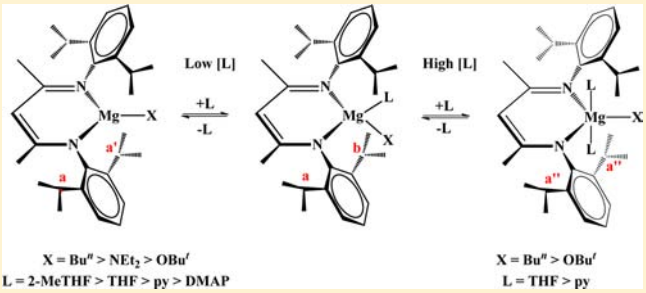

INTRODUCTION

Since their discovery well over a hundred years ago, the chemistry of alkyl-magnesium and −zinc reagents has continued to attract enormous attention due to their remarkable synthetic utility in organic syntheses. Solvation has long been known to dramatically alter reactivity, and alkyl-halides of magnesium and zinc are notoriously kinetically labile toward Schlenk equilibria involving ligand scrambling.[1] The addition of group 1 metal salts/complexes has recently added a new dimension of enhanced reactivity toward C−H activation by the Mg−R or Zn−R bonds as is now well established by Knochel and Mulvey in their separate schools of s-block chemistry.[2−9] Solvents and halides can be viewed as kinetically labile ligands in a solution phase, and thus, solid-state structures determined by single-crystal X-ray studies, though interesting in themselves, may shine little light on reactivity and solution behavior. The introduction of chelating anionic ligands may lead to a taming of these kinetically facile solution transformations. This was so elegantly demonstrated by Noyori in his chemical amplification of enantiomeric synthesis of alcohols employing mixtures of *R*- and *S*-ligated zinc alkyls.[10] This arose from the monomer−dimer equilibria in which the monomer was reactive and the *R*,*S*-dimer, which is favored thermodynamically in mixtures where both (*R*- and *S*-)LZnR complexes are present, was chemically inert.

We have been interested in the use of chelating ligands such as trispyrazolyl borate, Tp, and β-diketoiminates in s-block chemistry.[11−16] Sterically demanding Tp ligands, in general, seem to suppress the reactivity of Mg- and Zn-alkyls and -alkoxides relative to the commonly employed β-diketoiminate BDI ligand shown in Figure 1. This ligand has found extensive use both in transition metal and main group catalysis.[17−37]

In comparing the reactivity of closely related magnesium and zinc reagents, it can generally be concluded that magnesium is more reactive and kinetically labile. In a sense, zinc is softer and

Received: June 21, 2013
Published: September 25, 2013

   dx.doi.org/10.1021/ic401559b | Inorg. Chem. 2013, 52, 11302−11310

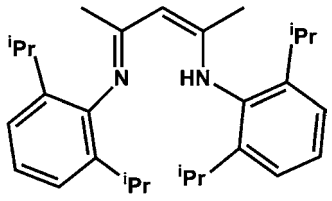

Figure 1. 2-[(2,6-Diisopropylphenyl)amino]-4-[(2,6-diisopropylphenyl)imino]pent-2-ene (BDIH).

forms more covalent bonds. In contrast, magnesium is harder and more oxophilic, and its bonds are primarily electrostatic or ionic. There is little or no directed valence: the geometry of a complex is largely determined by a combination of steric and electrostatic considerations.

We recently reported some of the reactions of the complex (BDI)MgBu^n(THF) and related alkyls.[38] This complex was an excellent initiator for the ring-opening polymerization, ROP, of the cyclic esters caprolactone, CL, and lactide, LA, to produce polycaprolactone, PCL, and polylactide, PLA, respectively. Indeed, in solution these polymerizations are among the most rapid that have been reported using magnesium complexes as an initiator. The rate of polymerization of CL, k_p =110 M^{-1} s^{-1}, was an order of magnitude faster than that of lactide polymerization, k_p = 10.7 M^{-1} s^{-1}, in toluene and CH_2Cl_2. For LA, the reaction occurs slower in THF relative to CH_2Cl_2 k_{app} = 0.10 s^{-1} and 0.42 s^{-1} in THF and CH_2Cl_2, respectively. However, while in the ROP of *rac*-LA in toluene or CH_2Cl_2 we observed formation of essentially atactic PLA, the reaction in THF at room temperature showed a marked preference for heterotactic PLA wherein the D- and L- forms of LA are enchained in a preferential sequential manner. The probability for this alternate enchainment of D- and L-LA, P_r, was 0.95. This influence of the solvent THF had been seen before in the ROP of *rac*-LA by coordinate catalysis, and an implication is that THF is intimately involved in the transition state leading to ring-opening. Rzepa, in a computational analysis of the ROP of LA by (BDI)Mg(OMe)(THF), implicated a 5-coordinate Mg^{2+} ion involving a coordinated THF molecule but not as the reason for this stereoselective polymerization of *rac*-LA to yield heterotactic PLA.[39] These calculations suggested that THF accelerated the rate of the ROP. Indeed, if THF was omitted from the calculations, the energy of activation was raised by ~10 kcal·mol^{-1} due to entropic factors. While solvents such as CH_2Cl_2 and toluene do not approximate to gas-phase reactions, the notable reaction rates as a function solvent, CH_2Cl_2 ~ toluene > THF, seemed to be puzzling. This caused us to examine the solution behavior of (BDI)MgBu^n(THF) in greater detail, particularly with respect to the lability of the coordinated THF molecule. In this paper we report the full details of the dynamics of THF self-exchange in the series (BDI)MgX(THF), where X = Bu^n, NEt_2, and OBu^t. These reveal some very interesting insights into the molecular dynamics and kinetic behavior of these molecules in solution. A preliminary report pertaining to the complex where X = Bu^n has been published.[40]

RESULTS AND DISCUSSION

Syntheses. The 2-methyltetrahydrofuran complex was made by the addition of 2-methyltetrahydrofuran, 2-MeTHF, to a hydrocarbon solution of (BDI)MgBu^n, yielding (BDI)-MgBu^n(2-MeTHF) as a white microcrystalline product. This procedure is directly analogous to the preparation of the THF complex. The amide complex (BDI)MgNEt$_2$(THF) and the alkoxide (BDI)MgOBu^t(THF) were made by the addition of

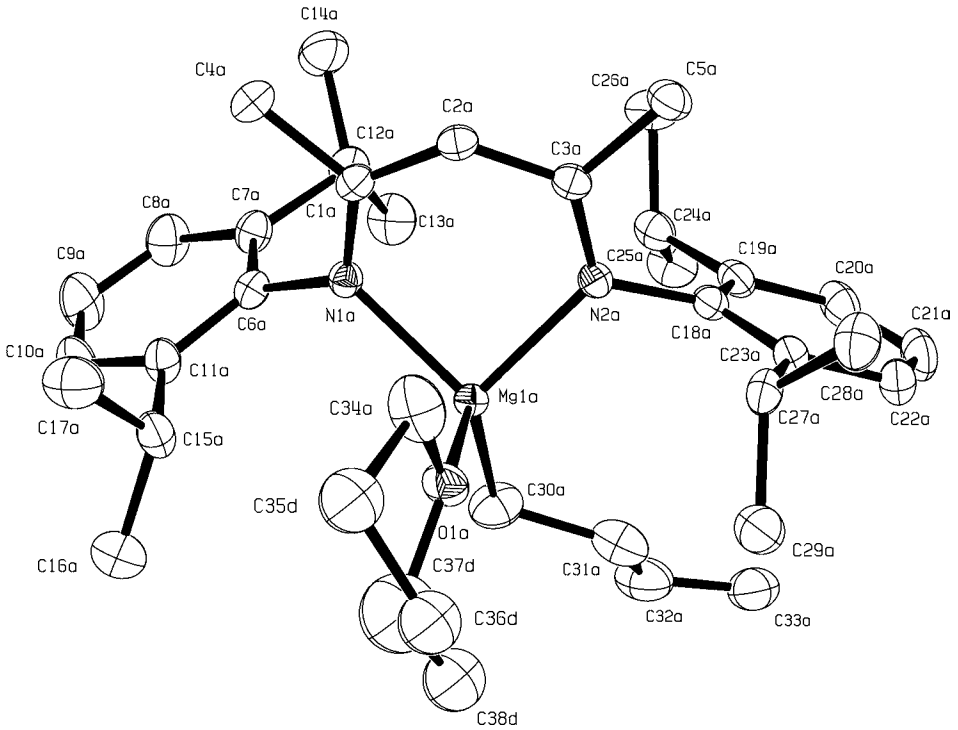

Figure 2. ORTEP drawing of (BDI)MgBu^n(2-MeTHF) with thermal ellipsoids drawn at the 30% probability level. The structure shows a distorted tetrahedral geometry around the Mg metal center. All hydrogen atoms are omitted for clarity. Only the major component of the disordered Me-THF ligand is shown.

dx.doi.org/10.1021/ic401559b | *Inorg. Chem.* 2013, 52, 11302−11310

diethylamine and *tert*-butanol, respectively, to (BDI)-MgBu^n(THF) in hexane.[14,38]

Crystal and Molecular Structure of (BDI)MgBu^n(2-MeTHF). The crystal and molecular structures of (BDI)-MgBu^n(THF)[38] and (BDI)MgOBu^t(THF)[14] have been previously determined, and the purpose of the synthesis of the 2-MeTHF adduct of the *n*-butyl complex was entirely to examine the influence of introducing the methyl group in terms of increasing steric pressure at the Mg^{2+} center. In the space group $P2_1/c$, both enantiomers are present in the unit cell. The asymmetric unit contains two independent molecules ($Z' = 2$), and the structure of one molecule is shown in Figure 2. Crystallographic details are reported in Table 1. The gross features of the structure are very similar to those of the THF adduct originally reported by Hill.[41] A comparison of the metric parameters involving the $MgN_2C(O)$ cores of the two complexes is given in Table 2.

Table 1. Crystallographic Details for (BDI)MgBu^n(2-MeTHF)

compound	(BDI)MgBu^n(2-MeTHF)
formula	$C_{38}H_{60}MgN_2O$
formula weight	585.19
temperature	150(2) K
wavelength	0.71073 Å
crystal system	monoclinic
space group	$P2_1/c$
unit cell dimensions	a = 15.7120(1) Å
	b = 24.1596(2) Å
	c = 19.3683(2) Å
	β = 98.971(1)°
volume	7262.19(11) Å^3
Z	8
density (calcd)	1.070 Mg/m^3
absorption coefficient	0.078 mm^{-1}
F(000)	2576
crystal size	0.19 × 0.38 × 0.46 mm^3
θ range for data collection	2.14 to 25.02°
index ranges	$-18 \le h \le 18$, $-28 \le k \le 28$, $-23 \le l \le 23$
reflections collected	99465
independent reflections	12793 [R(int) = 0.047]
completeness to θ = 25.02°	99.9%
refinement method	full-matrix least-squares on F^2
data/restraints/parameters	12793/14/773
goodness-of-fit on F^2	1.053
final R indices [$I > 2\sigma(I)$]	R1 = 0.0752, wR2 = 0.2017
R indices (all data)	R1 = 0.1135, wR2 = 0.2287
largest diff. peak and hole	0.896 and −0.499 e/Å^3
CCDC number	939830

The increased steric pressure in the 2-MeTHF complex has only a very small influence over the bond distances and angles. However, we do see that one of the N−Mg−O angles is enlarged and the Mg−N(2) and Mg−O distances are slightly larger in the 2-MeTHF complex: Mg−O(THF) = 2.058(1) Å and Mg−O(2-MeTHF) = 2.103(2) Å and 2.092(2) Å. As we show, these subtle changes translate to detectable changes in the kinetic lability of the two complexes.

THF or 2-MeTHF Exchange. Each of the complexes has been studied with respect to exchange with added THF or 2-MeTHF in toluene-d_8. The kinetics of exchange between the coordinated ligand and the free ligand was determined at various temperatures by line-shape analysis. In these experiments, the added free ligand (THF or 2-MeTHF) was varied from 0 to 2.5 equiv. This type of study does not lend itself to large excesses of added ligand; although, as we show later, the influence of added ligand in larger excess can be inferred from other dynamic NMR behavior. In the study of dynamic exchange between free and coordinated ligands, we have employed the use of both $^{13}C\{^1H\}$ and ^1H NMR spectroscopy. The observed and simulated line-shapes for THF exchange with the complex (BDI)MgBu^n(THF) were shown previously,[40] and related comparisons of the selected experimental and simulated spectra of (BDI)MgBu^n(2-MeTHF) are shown in Figure 3. The kinetics data of all complexes are provided in the Supporting Information.

The rates of 2-MeTHF exchange did not depend on the 2-MeTHF concentrations as shown in Figure 4. Similar results were also observed for the other title complexes. Thus, the simulated data for the ligand L exchange of all the complexes (X = Bu^n, NEt$_2$, and OBu^t) suggest that the ligand L exchanges via a dissociative process as shown in Figure 6. From the Eyring plots of $\ln(k/T)$ vs $1/T$, we can estimate the activation parameters for the dissociative process, which is observed as the only contributor to the dynamic exchange at low added THF or 2-MeTHF concentrations, as shown in Table 3, and the Eyring plot of (BDI)MgBu^n(2-MeTHF) is shown in Figure 5. For the complexes (BDI)MgX(THF), the $\Delta H^{\#}$ values follow the order X = OBu^t > NEt$_2$ > Bu^n, and for (BDI)MgBu^n(L), L = 2-MeTHF < THF. For the latter complex the exchange rate 2-MeTHF > THF is consistent with steric factors controlling the rate of a dissociation. For the series X = Bu^n, NEt$_2$, and OBu^t, we propose that the order Bu^n > NEt$_2$ > OBu^t is at least in part determined by the relative nucleophilicity of the ligand X. Alternatively expressed, the rate of dissociation of THF increases with the electronegativity of the atom bonded to Mg−O > Mg−N > Mg−C. Of course, the steric factors of the ligands differ, but it is clear that the dissociation of THF follows the order Bu^n > NEt$_2$ > OBu^t. Activation parameters are given in Table 3, and plots of ln k/T vs $1/T$ are given in the SI.

Apparent Aryl Group Rotation. In the preliminary communication of this work, we noted that the rate of apparent aryl rotation as monitored by the coalescence of the methine proton resonances of the isopropyl groups correlated with the rate of dissociation of the THF ligand in (BDI)-MgBu^n(THF). In the present study, we see that this holds true for the complexes (BDI)MgX(THF), where coalescence temperatures of the isopropyl ^{13}C methine and the α-methylene carbon of THF or 2-MeTHF resonances follow the order X = OBu^t (T_c = +15 °C) > NEt$_2$ (T_c = −5 °C) > Bu^n (T_c = −15 °C), as shown in Table 5. Furthermore, in the more kinetically labile 2-MeTHF complex, T_c is −45 °C. As shown in Table 4, the activation parameters for THF dissociation are within experimental error the same as those for apparent aryl group rotation. The rate of the apparent aryl ring rotation increases in the order in OBu^t, NEt$_2$, and Bu^n, which can qualitatively be estimated by the coalescence temperatures as shown in Table 5. Quantitatively, Table 6 shows the comparative simulated rates of this apparent aryl rotation at 27 °C, and all the simulated rates of apparent aryl rotation upon the addition of free THF are provided in the Supporting Information.

dx.doi.org/10.1021/ic401559b | Inorg. Chem. 2013, 52, 11302−11310

Table 2. Selected Bond Distances, Å, and Bond Angles, deg, for the Compounds (BDI)MgBu^n(THF) and (BDI)MgBu^n(2-MeTHF)

	distance	distance	angle	angle
atoms	THF	2-MeTHF	THF	2-MeTHF
Mg−N(1)	2.071(1)	2.074(2), 2.078(2)		
Mg−N(2)	2.063(1)	2.083(2), 2.079(2)		
Mg−C	2.127(2)	2.119(3), 2.130(4)		
Mg−O	2.058(1)	2.092(2), 2.103(2)		
N(1)−Mg−N(2)			93.00(5)	92.17(9), 92.41(9)
N(1)−Mg−C			119.20(7)	122.3(1), 116.7(2)
N(2)−Mg−C			126.40(7)	118.7(1), 126.0(1)
N(1)−Mg−O			102.55(5)	102,36(9), 102.20(9)
N(2)−Mg−O			101.31(5)	102.60(9), 102.7(1)
C−Mg−O			110.57(7)	114.8(1), 112.8 (1)

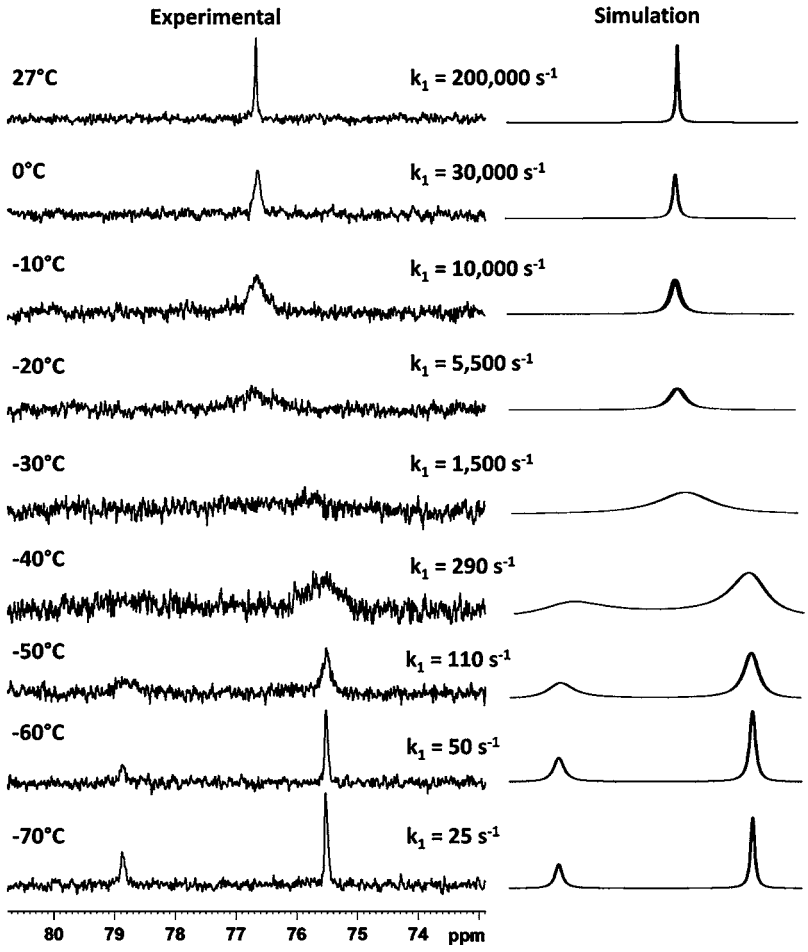

Figure 3. V.T ^{13}C 125 MHz NMR spectra of 0.035 M (BDI)MgBu^n(2-MeTHF) with 0.053 M 2-MeTHF (1:1.5) in toluene-d_8: experimental (left) and simulation (right). Only the α-methylene carbons in relation to the oxygen of 2-MeTHF are shown. The coordinated 2-MeTHF signal (left) downfield of the free 2-MeTHF (right). First -order rate constants and temperatures are shown on the left.

For a three-coordinate complex (BDI)MgX there would be a plane of symmetry which would make the Pr^i group on the aryl ligands equivalent as is seen in 3-coordinate zinc complexes of the form (BDI)ZnR. Therefore, the T_c values for the Pr^i ligands are better correlated with the dissociation of THF (or 2-MeTHF) than an aryl group rotation in a four-coordinate metal complex.

While apparent aryl rotation rates as obtained from averaging of the isopropyl resonances appear invariant with THF concentration up to 0.070 M (2 equiv), we observed that with larger additions of THF the apparent aryl rotation increases and the T_c values are lowered with an ultimate value in neat THF-d_8. In the case of (BDI)MgBu^n(THF) in toluene-d_8, the coalescence is significantly depressed until in neat THF-d_8 T_c = −75 °C (see Table 5), which qualitatively indicates the faster apparent aryl rotation. We do not have access to 2-MeTHF-d_{10}, so a similar study could not be performed, but we did observe that for X = OBu^t the T_c for apparent aryl rotation was suppressed from 15 °C in toluene-d_8 to −10 °C in THF-d_8. Equally significant is the observation that the coalescence

dx.doi.org/10.1021/ic401559b | Inorg. Chem. 2013, 52, 11302−11310

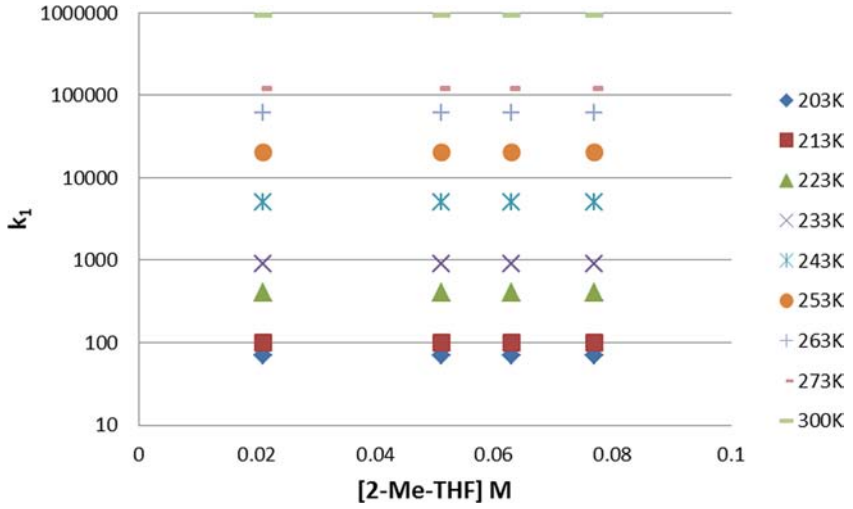

Figure 4. Plot of simulated k_1 for its exchange between free and coordinated sites vs [2-MeTHF] of 0.035 M (BDI)MgBu^n(2-MeTHF) in toluene-d_8, with various 2-MeTHF additions showing the independence in [2-MeTHF].

Table 3. Activation Parameters of the Dissociative Exchange Process of L in (BDI)MgX(L) Complexes, where X = Bu^n, NEt$_2$, OBu^t and L = THF and 2-MeTHF; [Mg] = 0.035 M in Toluene-d_8, with the Addition of L from 0.5−2.5 equiv

compd	L	$\Delta H^{\#}$ (kcal mol^{-1})	$\Delta S^{\#}$ (cal mol^{-1} K^{-1})
(BDI)MgBu^n(THF)	THF	13.4 ± 0.4	6.3 ± 1.6
(BDI)MgBu^n(2-MeTHF)	2-MeTHF	12.8 ± 0.5	8.6 ± 1.8
(BDI)MgOBu^t(THF)	THF	16.4 ± 0.3	9.5 ± 1.3
(BDI)MgNEt$_2$(THF)	THF	15.2 ± 0.5	9.2 ± 2.0

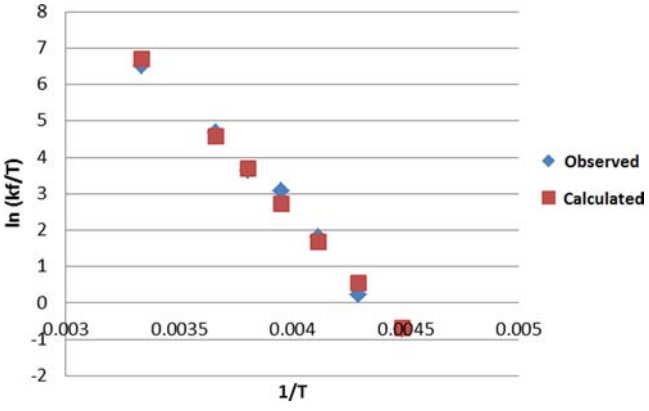

Figure 5. Eyring plot of the 2-MeTHF dissociation process in (BDI)MgBu^n(2-MeTHF); ($y = -6421.14x + 28.11$, $R^2 = 0.9919$).

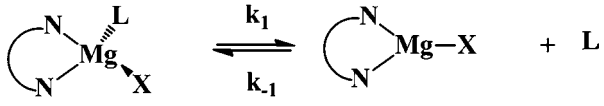

Figure 6. Proposed dissociative process of L involving (BDI)MgX(L), X = Bun, NEt$_2$, and OBu^t, L = 2-MeTHF and THF.

temperature for the complex where X = NEt$_2$ is invariant in toluene-d_8 and THF-d_8. A similar behavior is observed for the apparent aryl group rotation in compounds of the form (BDI)MgX(py) when the spectra are run in toluene-d_8 versus pyridine-d_5, and this will be described elsewhere. Thus, only

Table 4. Comparative Activation Parameters of the Dissociative Exchange Process of L and the Apparent Aryl Rotation in (BDI)MgX(L) Complexes[a]

	dissociative exchange of L		apparent aryl rotation	
compd	$\Delta H^{\#}$ (kcal mol^{-1})	$\Delta S^{\#}$ (cal mol^{-1} K^{-1})	$\Delta H^{\#}$ (kcal mol^{-1})	$\Delta S^{\#}$ (cal mol^{-1} K^{-1})
(BDI) MgBu^n(THF)	13.4 ± 0.4	6.3 ± 1.6	13.4 ± 0.5	5.3 ± 2.1
(BDI) MgOBu^t(THF)	16.4 ± 0.3	9.5 ± 1.3	16.8 ± 0.9	11.1 ± 3.2
(BDI) MgNEt$_2$(THF)	15.2 ± 0.5	9.2 ± 2.0	15.5 ± 0.6	11.4 ± 2.3

[a]X = Bu^n, NEt$_2$, OBu^t and L = THF; [Mg] = 0.035 M in toluene-d_8, with the addition of L from 0.5 to 2.5 equiv.

donor ligands appear to influence the rate of apparent aryl group rotation for certain complexes.

The ability of the donor ligand when present in a large excess to increase the rate of apparent aryl group rotation clearly indicates its noninnocent interaction with the metal complex. We propose that the most likely cause for this behavior lies in the ability of the donor to associate with the complex. One can envisage a five-coordinate structure based on a trigonal bipyramid as shown schematically in drawing **I**. In this activated

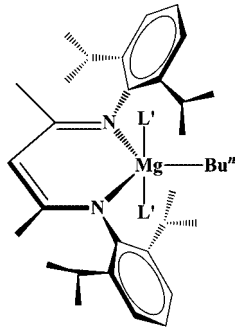

I

complex there is a mirror plane which causes an equivalence of the Pr^i ligands bound to the aryl groups. We note that the (BDI)Ca(BH$_4$)(THF)$_2$ complex reported by Mountford,[42] involving the larger Ca^{2+} ion, with an ionic radius of ∼1.0 Å

dx.doi.org/10.1021/ic401559b | Inorg. Chem. 2013, 52, 11302−11310

Table 5. Coalescence Temperatures for Apparent Aryl Rotation in the Compounds Estimated from $^{13}C\{^1H\}$ NMR Spectra Noted with Varying Equivalents of Added L; [M] = 0.035 M[a]

	coalescent temperature of Pr^i of aryl rotation (°C)							
compd	Tol-d_8	0.018 M	0.035 M	0.070 M	0.700 M	1.75 M	3.50 M	THF-d_8 (4.52M)
(BDI)MgBu^n(THF)	−15	−15	−15	−15	−40	−50	−65	−75
(BDI)MgBu^n(2-MeTHF)	−45	−45	−45	−45	nd	nd	nd	nd
(BDI)MgOBu^t(THF)	15	15	15	15	nd	10	nd	−10
(BDI)MgNEt$_2$(THF)	−5	−5	−5	−5	nd	−5	−5	−5

[a]nd = no data.

Table 6. Comparative Simulated Rates of the Apparent Aryl Ring Rotation in the Compounds Estimated from $^{13}C\{^1H\}$ NMR Line-Shape Analysis at 27°C Noted with Varying Equivalents of Added L; [M] = 0.035 M

	rate of the aryl rotation (s^{-1})							
compds	Tol-d_8	0.018 M	0.035 M	0.070 M	0.700 M	1.75 M	3.50 M	THF-d_8 (4.52 M)
(BDI)MgBu^n(THF)	20000	20000	20000	20000	27150	30000	55700	55700
(BDI)MgOBu^t(THF)	700	700	700	700	nd	1100	nd	1800
(BDI)MgNEt$_2$(THF)	10000	10000	10000	10000	nd	10000	10000	10000

compared to Mg^{2+} of ∼0.8 Å, has a similar structure if the BH_4^- ligand is considered to occupy a single coordination site. The coordination of the donor solvent would then lead to an interchange associative mechanism that competes at high donor solvent concentrations with the dissociative one observed at low donor concentrations. This situation is not uncommon for kinetically labile ions where the energy for activation for associative and dissociative interchange processes is similar.

Finally, we note that the "apparent aryl rotation" pertains only to the observations of the four-coordinated Mg^{2+} ion. In reality the dissociative or associative processes will head to equivalent Pr^i ligands on the aryl groups, and so the T_c values need not correlate with aryl rotation in a four-coordinate Mg^{2+} ion.

If we consider that, in neat THF-d_8, the rate of THF ligand exchange has a rate equivalent to that of the apparent aryl group rotation and we know that which is accounted for by the dissociative process at that temperature, then we can say that the total rate of THF exchange = $k_{dissociative}$[Mg] + $k_{associative}$[Mg][THF], as shown in Figure 9. From this we may get an estimate of the contribution of the associative interchange rate and an estimate of its activation parameters.

Focusing on the proposed associative mechanism process (see Figure 9) with the assumption that the apparent aryl group rotation correlates with THF exchange, the observed pseudo-first-order rate constant at higher concentration of THF is given by $k_{obs} = k_2$[THF]. The k_2 value at different temperatures and concentrations of THF was extracted, since k_{obs} and [THF] were known values. The k_2 values of (BDI)MgBu^n(THF) and (BDI)MgOBu^t(THF) are given in Tables 7 and 8, respectively. The independence of k_2 values from THF concentration is supportive of the associative process. The Eyring plots of (BDI)MgBu^n(THF) and (BDI)MgOBu^t(THF) are shown in Figures 7 and 8, respectively, and the activation parameters are given in Table 9.

We speculate that the lack of an observed interchange associative mechanism for the diethylamide complex is largely due to steric factors. The reader may wonder why we have not studied THF exchange with less bulky groups that more correlate with the Mg−Bu^n group i.e., where X = NHPr^n or OBu^n. The simple reason is that the respective THF complexes of those primary amides and alkoxides are not chemically persistent in solvents such as toluene. They are subject to facile ligand scrambling typical of Schlenk equilibria.

Table 7. Calculated k_2 of the THF Associative Process Involving 0.035 M (BDI)MgBu^n(THF) and the Different Added THF in Toluene-d_8[a]

	k_2		
temp (°C)	0.700 M free THF	1.750 M free THF	3.500 M free THF
−70	60	60	60
−60	150	150	150
−50	273	273	273
−40	535	535	535
−30	750	750	750
−20	1350	1350	1350
−10	2450	2450	2450
27	10000	10000	10000

[a]The obtained rates were based on the assumption that the apparent aryl group rotation correlates with THF exchange and the solvent effect on chemical shifts is not important.

Table 8. Calculated k_2 of the THF Associative Process Involving 0.035 M (BDI)MgOBu^t(THF) and the Different Added THF in Toluene-d_8[a]

	k_2	
temp (°C)	1.750 M free THF	4.515 M free THF
−30	7	7
−20	15	15
−10	43	43
0	69	69
27	229	229

[a]The obtained rates were based on the assumption that the apparent aryl group rotation correlates with THF exchange and the solvent effect on chemical shifts is not important.

THF Mg−O Bond Rotation. At very low temperatures in toluene-d_8, we also see from the $^{13}C\{^1H\}$ NMR spectra that the α-carbons of the bound THF ligands split into two signals of equal intensity for the complexes where X = NEt$_2$ and OBu^t. From the variable temperature spectra and the coalescence behavior of these signals, we can also estimate the activation parameters for this M−O bond rotation, and these are also listed in Table 10. For the complex, where X = Bu^n, this

dx.doi.org/10.1021/ic401559b | Inorg. Chem. 2013, 52, 11302−11310

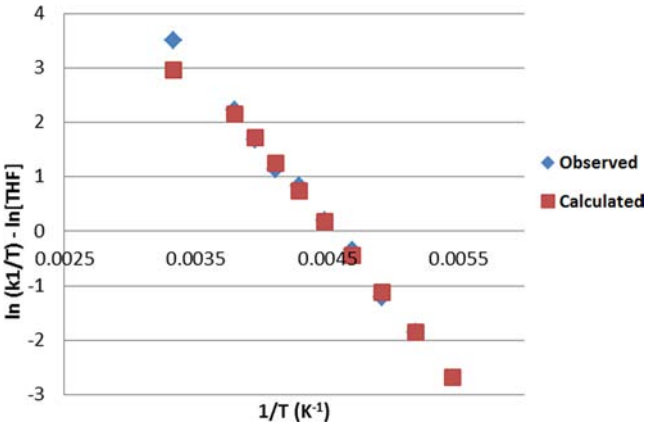

Figure 7. Eyring plot of the THF associative process involving 0.035 M (BDI)MgBu^n(THF) and added 1.750 M of free THF in toluene-d_8. The activation parameters are approximate and based on the assumption that the apparent aryl group rotation correlates with THF exchange and the solvent effect on chemical shifts is not important. (y = −2919.68x + 13.25, R^2 = 0.99).

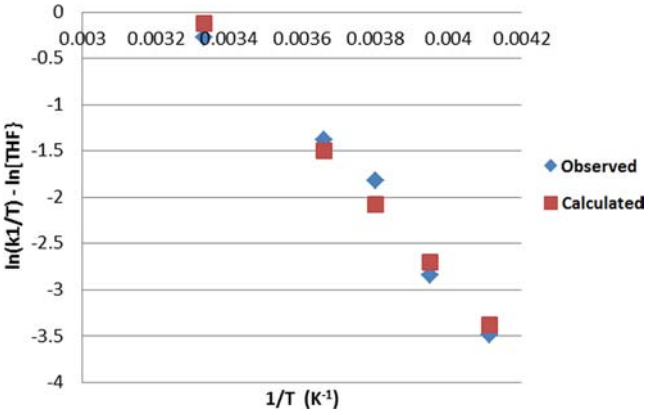

Figure 8. Eyring plot of the THF associative process involving 0.035 M (BDI)MgOBu^t(THF) and added 1.750 M of free THF in toluene-d_8. The activation parameters are approximate and based on the assumption that the apparent aryl group rotation correlates with THF exchange and the solvent effect on chemical shifts is not important. (y = −4179.60x + 13.76, R^2 = 0.98).

Dissociative Process

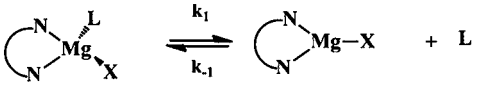

Associative Process

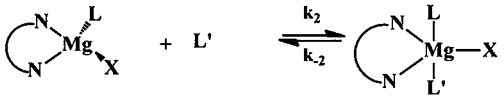

$$\text{rate} = k_1[(\text{BDI})\text{MgX(L)}] + k_2[(\text{BDI})\text{MgX(L)}][\text{L}]$$

Figure 9. Dissociative and associative reactions of L exchange that contribute to the total rate of L exchange in the presence of a large excess of added L.

rotation seemingly cannot be frozen out even at −100 °C. Baring the accidental degeneracy of the α-carbons of the bound THF molecule, our suggestion is that the less sterically demanding Mg−Bu^n group has an even smaller barrier to Mg−O rotation when compared to X = NEt$_2$ and OBu^t.

Table 9. Activation Parameters of the Associative Exchange Process of L in (BDI)MgX(L) Complexes, Where X = Bu^n, NEt$_2$, OBu^t and L = THF; [Mg] = 0.035 M

	dissociative exchange of L	
compd	$\Delta H^{\#}$ (kcal mol^{-1})	$\Delta S^{\#}$ (cal mol^{-1} K^{-1})
(BDI)MgBu^n(THF)	5.4 ± 0.1	−20.9 ± 0.3
(BDI)MgOBu^t(THF)	8.3 ± 0.8	−19.8 ± 3.0
(BDI)MgNEt$_2$(THF)		

Table 10. Activation Parameters of the Bonded THF Rotation in (BDI)MgX(L), Where X = Bu^n, NEt$_2$, OBu^t and L = THF; [Mg] = 0.035 M

compd	$\Delta H^{\#}$ (kcal mol^{-1})	$\Delta S^{\#}$ (cal mol^{-1} K^{-1})
(BDI)MgBu^n(THF)	too fast	too fast
(BDI)MgOBu^t(THF)	6.9 ± 0.1	−13.4 ± 0.4
(BDI)MgNEt$_2$(THF)	5.0 ± 0.1	−24.8 ± 0.4

CONCLUDING REMARKS

The present study reveals some interesting insights into the kinetic lability of a bound THF ligand at a Mg^{2+} center supported by the chelating BDI ligand as a function of the Mg−X bond, where X = an alkyl, an amide, and an alkoxide. The key question that remains is how this knowledge translates to an understanding of the solvent's role in the ring-opening of cyclic esters such as lactide or caprolactone. While this is a matter of continuing investigation, we do note here that the points of onset of polymerization by the complexes where X = Bu^n, NEt$_2$, and OBu^t in toluene-d_8 in the presence of 5 equiv of LA differ. It is, however, worth noting that the ring-opening event involves attack on the carbonyl carbon of a bond LA molecule by the amide nitrogen or the oxygen of the alkoxide whereas for the Bu^n group the initiation step involves a β-hydrogen atom transfer via a six-membered transition state with the ultimate expulsion of 1-butene. Thus, any direct correlation between the initial rate of ring-opening and the rate of THF dissociation need not be valid. However, it is by studies such as these that we may expect to discover important insights into the mechanisms of the reactions of these kinetically labile complexes of Mg^{2+} and their role in organic transformations and catalysis.

EXPERIMENTAL SECTION

All the reactions were handled under a N$_2$ atmosphere employing Schlenk line and drybox techniques. Tetrahydrofuran, hexane, toluene, and pentane were distilled under nitrogen from calcium hydride. 1 M di-*n*-butylmagnesium in pentane, 2-MeTHF, and HNEt$_2$ were purchased from Sigma-Aldrich. Deuterated toluene and THF were purchased from Cambridge Isotope Laboratory. 2-MeTHF, toluene-d_8, and THF-d_8 were distilled under a N$_2$ atmosphere from calcium hydride and stored over 4 Å molecular sieves overnight prior to use. The solutions were made inside a glovebox under a nitrogen atmosphere and transferred to a J-Young NMR tube. The β-diiminato ligand (2-[(2,6-diisopropylphenyl)amino]-4-[(2,6-diisopropylphenyl)-imino]pent-2-ene) (BDIH),[43] (BDI)MgBu^n(THF),[38] and (BDI)-MgOBu^t(THF),[14] was prepared according to the literature procedures.

Measurement. *NMR Spectroscopy.* Variable temperature ^{1}H and ^{13}C NMR spectra from 183 K to 373K were acquired on a Bruker DPX-500 NMR spectrometer using a J-Young NMR tube. The temperature of the probe was adjusted with a standard temperature-

dx.doi.org/10.1021/ic401559b | Inorg. Chem. 2013, 52, 11302−11310

control unit, using a heating element under air atmosphere at high temperature and liquid nitrogen under a nitrogen atmosphere at low temperature. Pure methonal and 80% ethylene glycol in DMSO were used to calibrate the probe temperature for low and high temperature, respectively.[44,45] The accuracy of the temperature measurement was ±0.5 °C. The probe was tuned at each temperature, and the sample tubes were left in the probe to achieve the thermal equilibrium for at least 15 min before taking measurements. The spectra were referenced by the residual protio impurity of toluene-d_8 at 2.08 ppm (^{1}H NMR) and 137.86 ppm (^{13}C NMR), THF-d_8 at 3.58 ppm (^{1}H NMR) and 67.57 ppm (^{13}C NMR), and py-d_5 at 8.74 ppm (^{1}H NMR) and 150.35 ppm (^{13}C NMR).

Line-Shape Analysis. The appearance of (BDI)MgBu^n(THF) NMR spectra over a temperature range suggests the molecules are probably undergoing the exchange of THF between its free and bound states by either one-step mutual exchange reaction without an intermediate step or a two-step process which involves a dissociative or an associative reaction. With this information in mind, simulations of these carbon spectra were carried out. The simulated spectra were compared with the experimental data. The simulated rate constant for the forward reaction k_f and the reverse reaction k_r do not show any monotonicity in regard to the variation of temperatures. This is inconsistent with the Eyring equation unless there is a second process that we have not considered or the assumptions for the simulation were inappropriate. Consequently, we have developed a new procedure which does not require any assumptions on the dynamic functional form to study the spectra. We call this the CCCF procedure, and it is described thoroughly in the Supporting Information.

This procedure provides us the following information:

1. The mean lifetime of the reactant is concentration independent, and it is equal to the inverse of forward rate constant k_f.
2. The reverse rate constant k_r is proportional to the (BDI)-MgBu^n(THF) concentration, and it is also inversely proportional to the concentration of the free THF.
3. The high temperature spectra also support the information listed in point 2.

Hence the reaction suggested by the analysis is

$$\text{(BDI)MgBu}^n\text{(THF)} \rightleftharpoons \text{(BDI)MgBu}^n + \text{THF}$$

In addition, we need to address the unobservable carbon signal of (BDI)MgBu^n. From the steady state condition and the information provided by the simulation, we can conclude that the concentration of (BDI)MgBu^n is much less than 1 and the k_r is very large. This suggests that the mean lifetime of (BDI)MgBu^n is very short and the reverse reaction is very fast. So the carbon signal does not show up in the spectra. Spectral Analysis program is used for all the simulations.

Crystallography. Single-crystal X-ray diffraction data were collected on a Nonius KappaCCD diffractometer at low temperature using an Oxford Cryosystems Cryostream Cooler. The crystals were coated with a Fomblin oil due to their air-sensitive nature. A combination of ψ and ω scans with a frame width of 1° was used for the data collection. Data integration was done with Denzo,[46] and scaling and merging of the data was done with Scalepack.[46] The structure was solved by direct methods in SHELXS-97.[47] Full-matrix least-squares refinements based on F^2 were performed in SHELXL-97,[47] as incorporated in the WinGX package.[48] Neutral atom scattering factors were used and include terms for anomalous dispersion.[49] There are two Mg complexes in the asymmetric unit, and they are labeled as A and B. The methyl-THF ligand is disordered over two sites in both molecules. For molecule A, atoms O(1A) and C(34A) are common to both sites, while there are two positions for each of the other atoms: C(35A), C(35D), C(36A), C(36D), C(37A), C(37D), C(38A), and C(38D). For molecule B, atoms O(1B), C(34B), C(35B), and C(38B) are common to both sites, while there are two positions for each of the other atoms: C(36B), C(36C), C(37B), and C(37C). These disordered atoms were refined only isotropically, and it was necessary to use distance restraints in the refinement of this model. For each methyl group, the hydrogen atoms were added at calculated positions using a riding model with U(H) = 1.5U_{eq}(bonded carbon atom). For the methyl groups in the chelating ligand, the torsion angle which defines the orientation of the methyl group about the C−C bond was refined. The rest of the hydrogen atoms were included in the model at calculated positions using a riding model with U(H) = 1.2U_{eq}(bonded atom).

Synthesis. (BDI)MgBu^n(2-MeTHF). To a solution of BDIH (1 g, 2.39 mmol) in 30 mL of hexane was slowly added 2.70 mL of 1 M MgBu$^n_2$ (2.70 mmol) in pentane. The solution was stirred at room temperature for 1 h, and then 0.40 mL of 2-MeTHF (4.00 mmol) was added. White solids immediately precipitated out of the solution. The solution was concentrated and cooled to −20 °C overnight. The white solid was collected after the filtration; then it was washed with pentane twice and dried under a dynamic vacuum to give the title compound in 88% yield. Crystals were collected from the concentrated solution of this compound in hexane. ^{1}H NMR (400 MHz, toluene-d_8, 27 °C): 7.11 (m, 6H, ArH), 4.78 (s, 1H, β-CH), 4.12 (m, 1H, 2-MeTHF), 3.66 (m, 1H, 2-MeTHF), 3.60 (m, 1H, 2-MeTHF), 3.34 (sept, 4H, J_{HH} = 6.92 Hz, C*H*MeMe′), 1.63 (s, 6H, α-Me), 1.49 (m, 2H, β-Bu^n), 1.35 (m, 4H, 2-MeTHF), 1.30 (d, 12H, J_{HH} = 6.92 Hz, CH*Me*$_2$), 1.23 (d, 12H, J_{HH} = 6.92 Hz, CH*Me*$_2$′), 1.00 (m, 2H, γ-Bu^n), 0.94 (t, 3H, J_{HH} = 7.22 Hz, δ-Bu^n), 0.87 (d, 3H, J_{HH} = 6.30 Hz, 2-MeTHF), −0.35 (AA′XX′Y, 2H, α-Bu^n). ^{13}C NMR (500 MHz, toluene-d_8): 168.71 (C═N), 146.63 (*ipso*-Ar), 142.90 (*o*-Ar), 125.61 (*p*-Ar), 124.25 (*m*-Ar), 95.41 (β-C), 78.53 (2-MeTHF), 69.75 (2-MeTHF), 33.02 (δ-Bu^n), 32.89 (γ-Bu^n), 32.50 (2-MeTHF), 28.60 (*C*HMe$_2$), 25.57 (2-MeTHF), 25.44 (CH*Me*$_2$), 25.02 (α-Me), 24.68 (CH*Me*$_2$), 14.88 (β-Bu^n), 7.67 (α-Bu^n).

(BDI)MgNEt$_2$(THF). To the solution of (BDI)MgBu^n(THF) (1 g, 1.75 mmol) in 20 mL of toluene was slowly added 0.22 mL of HNEt$_2$ (2.10 mmol). The reaction was stirred for 20 min; then all volatile components were removed under a dynamic vacuum, yielding a yellowish compound. The yellowish solids were then washed with 10 mL of pentane twice and dried under a dynamic vacuum, giving the title compound in 90% yield. ^{1}H NMR (400 MHz, toluene-d_8, 27 °C): 7.11 (m, 6H, ArH), 4.77 (s, 1H, β-CH), 3.70 (m, 4H, THF), 3.30 (br, 4H, C*H*MeMe′), 2.82 (q, 2H, J_{HH} = 6.83 Hz, NEt$_2$), 1.63 (s, 6H, α-Me), 1.34 (m, 4H, THF), 1.31 (d, 12H, J_{HH} = 6.92 Hz, CH*Me*$_2$), 1.22 (d, 12H, J_{HH} = 6.92 Hz, CH*Me*$_2$′), 0.80 (d, 3H, J_{HH} = 6.83 Hz, NEt$_2$). ^{13}C NMR (500 MHz, toluene-d_8): 168.82 (C═N), 146.96 (*ipso*-Ar), 142.89 (*o*-Ar), 125.78 (*p*-Ar), 124.26 (*m*-Ar), 95.10 (β-C), 70.50 (THF), 48.55 (β-NEt$_2$), 28.69 (*C*HMe$_2$), 25.74 (THF), 25.26 (CH*Me*$_2$), 25.06 (α-Me), 24.81 (CH*Me*$_2$), 18.64 (α- NEt$_2$).

■ ASSOCIATED CONTENT

Ⓢ Supporting Information

Lists of details of the line-shape analysis programs, simulations, kinetics data, Eyring plots, and crystallography. This material is available free of charge via the Internet at http://pubs.acs.org.

■ AUTHOR INFORMATION

Corresponding Authors

*E-mail: chisholm@chemistry.ohio-state.edu.

*E-mail: fraenkel@mps.ohio-state.edu.

Notes

The authors declare no competing financial interest.

■ ACKNOWLEDGMENTS

We thank the Department of Energy, Basic Chemical Sciences Division and National Science Foundation (NSF No. 1058035) for financial support. K.C. thanks the Royal Thai Government for a scholarship.

■ REFERENCES

(1) Schlenk, W.; Schlenk, W. J. *Ber. Dtsch. Chem. Ges.* **1929**, *62B*, 920−924.

(2) Krasovskiy, A.; Knochel, P. *Angew. Chem., Int. Ed.* **2004**, *43*, 3333−3336.

(3) Blasberg, F.; Bolte, M.; Wagner, M.; Lerner, H.-W. *Organometallics* **2012**, *31*, 1001−1005.
(4) Mulvey, R. E. *Acc. Chem. Res.* **2009**, *42*, 743−755.
(5) Armstrong, D. R.; García-Álvarez, P.; Kennedy, A. R.; Mulvey, R. E.; Parkinson, J. A. *Angew. Chem., Int. Ed.* **2010**, *49*, 3185−3188.
(6) Stoll, A. H.; Krasovskiy, A.; Knochel, P. *Angew. Chem., Int. Ed.* **2006**, *45*, 606−609.
(7) Krasovskiy, A.; Straub, B. F.; Knochel, P. *Angew. Chem., Int. Ed.* **2006**, *45*, 159−162.
(8) Krasovskiy, A.; Krasovskaya, V.; Knochel, P. *Angew. Chem., Int. Ed.* **2006**, *45*, 2958−2961.
(9) Krasovskiy, A.; Tishkov, A.; del Amo, V.; Mayr, H.; Knochel, P. *Angew. Chem., Int. Ed.* **2006**, *45*, 5010−5014.
(10) Kitamura, M.; Suga, S.; Niwa, M.; Noyori, R.; Zhai, Z.-X.; Suga, H. *The Journal of Physical Chemistry* **1994**, *98*, 12776−12781.
(11) Chisholm, M. H.; Gallucci, J. C.; Phomphrai, K. *Inorg. Chem.* **2005**, *44*, 8004−8010.
(12) Chisholm, M. H. *Pure Appl. Chem.* **2010**, *82*, 1647−1662.
(13) Chisholm, M. H.; Phomphrai, K. *Inor. Chim. Acta.* **2003**, *350*, 121−125.
(14) Chisholm, M. H.; Gallucci, J.; Phomphrai, K. *Inorg. Chem.* **2002**, *41*, 2785−2794.
(15) Chisholm, M. H.; Eilerts, N. W.; Huffman, J. C.; Iyer, S. S.; Pacold, M.; Phomphrai, K. *J. Am. Chem. Soc.* **2000**, *122*, 11845−11854.
(16) Chisholm, M. H.; Huffman, J. C.; Phomphrai, K. *J. Chem. Soc., Dalton Trans.* **2001**, *2001*, 222−224.
(17) Kim, W.-K.; Fevola, M. J.; Liable-Sands, L. M.; Rheingold, A. L.; Theopold, K. H. *Organometallics* **1998**, *17*, 4541−4543.
(18) Oguadinma, P. O.; Schaper, F. *Organometallics* **2009**, *28*, 4089−4097.
(19) Bernskoetter, W. H.; Lobkovsky, E.; Chirik, P. J. *Organometallics* **2005**, *24*, 6250−6259.
(20) Bernskoetter, W. H.; Lobkovsky, E.; Chirik, P. J. *Organometallics* **2005**, *24*, 4367−4373.
(21) Tonzetich, Z. J.; Héroguel, F.; Do, L. H.; Lippard, S. J. *Inorg. Chem.* **2011**, *50*, 1570−1579.
(22) Latreche, S.; Schaper, F. *Organometallics* **2010**, *29*, 2180−2185.
(23) West, N. M.; White, P. S.; Templeton, J. L.; Nixon, J. F. *Organometallics* **2009**, *28*, 1425−1434.
(24) Bai, G.; Wei, P.; Das, A.; Stephan, D. W. *Organometallics* **2006**, *25*, 5870−5878.
(25) Basuli, F.; Huffman, J. C.; Mindiola, D. J. *Inorg. Chem.* **2003**, *42*, 8003−8010.
(26) Hamaki, H.; Takeda, N.; Tokitoh, N. *Organometallics* **2006**, *25*, 2457−2464.
(27) Bai, G.; Wei, P.; Stephan, D. W. *Organometallics* **2006**, *25*, 2649−2655.
(28) Budzelaar, P. H. M.; Moonen, N. N. P.; Gelder, R. de; Smits, J. M. M.; Gal, A. W. *Eur. J. Inorg. Chem.* **2000**, *2000*, 753−769.
(29) Rieth, L. R.; Moore, D. R.; Lobkovsky, E. B.; Coates, G. W. *J. Am. Chem. Soc.* **2002**, *124*, 15239−15248.
(30) Budzelaar, P. H. M.; Moonen, N. N. P.; de Gelder, R.; Smits, J. M. M.; Gal, A. W. *Chem.—Eur. J.* **2000**, *6*, 2740−2747.
(31) Hardman, N. J.; Wright, R. J.; Phillips, A. D.; Power, P. P. *J. Am. Chem. Soc.* **2003**, *125*, 2667−2679.
(32) Wei, X.; Cheng, Y.; Hitchcock, P. B.; Lappert, M. F. *Dalton Trans.* **2008**, 5235.
(33) Hadzovic, A.; Song, D. *Inorg. Chem.* **2008**, *47*, 12010−12017.
(34) Bernskoetter, W. H.; Lobkovsky, E.; Chirik, P. J. *Chem. Commun.* **2004**, 764−765.
(35) Hadzovic, A.; Song, D. *Organometallics* **2008**, *27*, 1290−1298.
(36) Bai, G.; Wei, P.; Stephan, D. W. *Organometallics* **2005**, *24*, 5901−5908.
(37) Budzelaar, M.; H, P.; Oort, V.; Bart, A.; Orpen, A. G. *Eur. J. Inorg. Chem.* **1998**, *1998*, 1485−1494.
(38) Chisholm, M. H.; Choojun, K.; Gallucci, J. C.; Wambua, P. M. *Chem. Sci.* **2012**, *3*, 3445−3457.
(39) Marshall, E. L.; Gibson, V. C.; Rzepa, H. S. *J. Am. Chem. Soc.* **2005**, *127*, 6048−6051.
(40) Chisholm, M. H.; Choojun, K.; Chow, A. S.; Fraenkel, G. *Angew. Chem., Int. Ed.* **2013**, *52*, 3264−3266.
(41) Hill, M. S.; MacDougall, D. J.; Mahon, M. F. *Dalton Trans.* **2010**, *39*, 11129−11131.
(42) Collins, R. A.; Unruangsri, J.; Mountford, P. *Dalton Trans.* **2012**, *42*, 759−769.
(43) Feldman, J.; McLain, S. J.; Parthasarathy, A.; Marshall, W. J.; Calabrese, J. C.; Arthur, S. D. *Organometallics* **1997**, *16*, 1514−1516.
(44) Van Geet, A. L. *Anal. Chem.* **1970**, *42*, 679−680.
(45) Raiford, D. S.; Fisk, C. L.; Becker, E. D. *Anal. Chem.* **1979**, *51*, 2050−2051.
(46) Otwinowski, Z.; Minor, W. In *Methods in Enzymology*; Charles, W. Carter, J., Ed.; Academic Press, 1997; Vol. *276*, pp 307−326.
(47) Sheldrick, G. M. *Acta Crystallogr.* **2008**, *A64*, 112−122.
(48) Farrugia, L. J. *J. Appl. Crystallogr.* **1999**, *32*, 837−838.
(49) Wilson, A. J. C. *International Tables for Crystallography, Vol. C: Mathematical, Physical and Chemical Tables*; 2nd ed.; Kluwer Academic Publishers, 1995.